Cell

Diabetes Risk Gene and Wnt Effector *Tcf7l2*/TCF4 Controls Hepatic Response to Perinatal and Adult Metabolic Demand

Sylvia F. Boj,[1] Johan H. van Es,[1] Meritxell Huch,[1] Vivian S.W. Li,[1] Anabel José,[2,3] Pantelis Hatzis,[1,7] Michal Mokry,[1] Andrea Haegebarth,[1,8] Maaike van den Born,[1] Pierre Chambon,[4] Peter Voshol,[5] Yuval Dor,[6] Edwin Cuppen,[1] Cristina Fillat,[2,3] and Hans Clevers[1,*]

[1]Hubrecht Institute, KNAW and University Medical Center Utrecht, 3584CT Utrecht, The Netherlands
[2]Centro de Investigación Biomédica en Red de Enfermedades Raras (CIBERER), 08036 Barcelona, Spain
[3]Institut d'Investigacions Biomèdiques August Pi i Sunyer-IDIBAPS, 08036 Barcelona, Spain
[4]Institut de Genetique et de Biologie Moleculaire et Cellulaire (IGBMC), Universite Louis Pasteur, 67404 Illkirch-Cedex, France
[5]Institute of Metabolic Science, Addenbrooke's Hospital, University of Cambridge, CB2 0QQ Cambridge, UK
[6]The Institute for Medical Research Israel-Canada, The Hebrew University-Hadassah Medical School, 91120 Jerusalem, Israel
[7]Present address: Biomedical Sciences Research Center Alexander Fleming, 16672 Vari, Greece
[8]Present address: Bayer Healthcare AG, 13353 Berlin, Germany
*Correspondence: h.clevers@hubrecht.eu
http://dx.doi.org/10.1016/j.cell.2012.10.053

SUMMARY

Most studies on *TCF7L2* SNP variants in the pathogenesis of type 2 diabetes (T2D) focus on a role of the encoded transcription factor TCF4 in β cells. Here, a mouse genetics approach shows that removal of TCF4 from β cells does not affect their function, whereas manipulating TCF4 levels in the liver has major effects on metabolism. In *Tcf7l2*$^{-/-}$ mice, the immediate postnatal surge in liver metabolism does not occur. Consequently, pups die due to hypoglycemia. By combining chromatin immunoprecipitation with gene expression profiling, we identify a TCF4-controlled metabolic gene program that is acutely activated in the postnatal liver. In concordance, adult liver-specific *Tcf7l2* knockout mice show reduced hepatic glucose production during fasting and display improved glucose homeostasis when maintained on high-fat diet. Furthermore, liver-specific TCF4 overexpression increases hepatic glucose production. These observations imply that TCF4 directly activates metabolic genes and that inhibition of Wnt signaling may be beneficial in metabolic disease.

INTRODUCTION

Wnt signaling controls virtually every aspect of embryonic development and mediates homeostatic self-renewal in adult tissues (Clevers and Nusse, 2012). When Wnt ligands bind to the Frizzled-Lrp5/6 receptor complex, it results in the stabilization and subsequent nuclear translocation of β-catenin. In the nucleus, stabilized β-catenin binds to TCF transcription factors to regulate the transcription of Wnt target genes.

Epidemiological evidence suggests that Wnt signaling may also play a role in metabolic disorders. Grant and colleagues identified a strong association between T2D risk and intronic SNPs in *TCF7L2* (Grant et al., 2006). Many follow-up studies have confirmed this discovery (Cauchi et al., 2007; Elbein et al., 2007; Florez et al., 2006). Individuals with variants of *TCF7L2* associated with increased risk for T2D show impaired insulin secretion (Florez et al., 2006; Saxena et al., 2006) and present an increased hepatic glucose production in fasting (Lyssenko et al., 2007).

Tcf7l2 mutant mice, which die in the immediate postnatal period, do not maintain stem cells in their intestinal crypts (Korinek et al., 1998). Moreover, the encoded TCF4 transcription factor activates the oncogenic program that is aberrantly activated in APC mutant colon cancer cells (Korinek et al., 1997; van de Wetering et al., 2002). In a recent study by Nobrega and colleagues, copy numbers of *Tcf7l2* were varied by transgenesis. Increased copy numbers of *Tcf7l2* rendered mice glucose intolerant, whereas decreasing gene copy numbers resulted in enhanced glucose tolerance (Savic et al., 2011). These observations imply that the human risk alleles of *TCF7L2* represent gain-of-function alleles for an as-yet-undefined role of TCF4 in metabolic control. Here, we address the tissue of action and the molecular mechanism of metabolic control by TCF4 by using mouse models allowing constitutive knockout, tissue-specific knockout, and transient overexpression of *Tcf7l2*.

RESULTS

Deletion of *Tcf7l2* in Insulin-Producing Cells Does Not Cause β Cell Dysfunction

The association of *TCF7L2*/TCF4 with T2D prompted us to compare *Tcf7l2* heterozygous with wild-type (WT) mice, addressing the possible role of TCF4 in metabolic regulation. We observed a difference in their body weight, with *Tcf7l2*$^{+/-}$ mice displaying more than 20% lower body weight compared to WT

littermates. TCF4 heterozygosity reduces glucose, insulin, fatty acid, triglyceride, and cholesterol levels in adult mice (data not shown). *Tcf7l2*$^{+/-}$ mice also have increased insulin sensitivity, improved glucose tolerance, and reduced capacity to produce glucose after pyruvate injection, even when they are fed with a 45% high-fat (HF) diet (data not shown), confirming previous observations (Savic et al., 2011).

Human carriers of the risk variants for *TCF7L2* reportedly display impaired insulin secretion (Florez et al., 2006; Saxena et al., 2006). We generated a *Tcf7l2* allele with *loxP* sites flanking exon 10 (van Es et al., 2012), which encodes the DNA-binding HMG box (Korinek et al., 1998). *Tcf7l2*$^{loxP/+}$ mice were bred with the tamoxifen-inducible pancreatic β-cell-specific Cre recombinase strain *RIP-Cre-ER*^{T2} (Dor et al., 2004). Because we did not observe any difference between the three controls (*Tcf7l2* $^{loxp/loxp}$, *RIP-Cre-ER*^{T2}, and WT) in body weight, blood glucose and plasma insulin levels, glucose tolerance test, and insulin secretion in vivo in the initial experiments (Figures S1A–S1E available online), we decided to use in the follow-up experiments *Tcf7l2*$^{loxp/loxp}$; RIP-Cre-ER^{T2} (βTCF4KO) and *Tcf7l2*$^{loxp/loxp}$ as control mice. Both groups of mice were injected with tamoxifen at weaning and were analyzed at the age of 2 to 3 months.

PCR and real-time RT-PCR were performed to quantify recombination of the *Tcf7l2* locus and depletion of *Tcf7l2* messenger RNA (mRNA) in β cells. As shown in Figure S2A, a single 1,132 bp band was observed in islets from controls. In contrast, by using DNA prepared from islets from βTCF4KO mice, the major product was 611 bp, indicating exon 10 deletion. *Tcf7l2* mRNA was strongly reduced in isolated islets from βTCF4KO mice (Figure 1K). The remaining *Tcf7l2* mRNA can be accounted for by the fact that β cells only make up ~80%–85% of islets.

We compared a set of metabolic parameters between adult βTCF4KO mice and control littermates on normal chow (NC) diet (Figure 1). Surprisingly, βTCF4KO mice were able to maintain euglycemia as compared to control littermates in the fed and the fasted state (Figure 1A). We did not detect any difference either in plasma insulin levels (Figure 1B) or in the ratio insulin/glucose (Figure 1C) in both states. When mice were exposed to a 45% HF diet (Figure S2), we observed no differences in body weight, gain of body weight, food intake, blood glucose, and plasma insulin levels between βTCF4KO and control mice (Figures S2B–S2G). To characterize physiological responses to glucose load, βTCF4KO and control mice on either NC (Figure 1D) or HF (Figure S2H) diet were subjected to an intraperitoneal (i.p.) glucose tolerance test after a 16 hr fast. This revealed no difference in glucose tolerance on either NC (Figure 1D) or HF (Figure S2H) diet. When mice on either NC (Figure 1E) or HF (Figure S2I) diet were injected with insulin to test their insulin tolerance, we did not observe any difference between both genotypes.

Then, insulin release was measured in response to glucose stimulation in vivo. The increase in plasma insulin levels 15 min after i.p. glucose injection did not differ between βTCF4KO and control mice on either NC (Figure 1F) or HF diet (Figure S2J). We also isolated pancreatic islets from βTCF4KO and control mice on either NC (Figure 1G) or HF (Figure S2K) diet for 8 weeks and tested insulin secretion in vitro. Under both feeding conditions, insulin release was equal at low (1.6 mM) and high (16.7 mM) glucose concentrations between βTCF4KO and control mice. Total insulin content did not differ between islets isolated from βTCF4KO and control mice in both feeding conditions (Figures 1H and S2L). Accordingly, histological analysis revealed no differences in pancreatic islets and in β cell mass (Figure 1I). Ki67 staining also revealed no effect of TCF4 deletion on β cell proliferation (Figure 1J).

We also measured the mRNA levels of genes relevant for maintaining β cell function in isolated pancreatic islets. As expected, *Tcf7l2* mRNA levels were dramatically reduced in the pancreatic islets of βTCF4KO mice ($p < 0.01$) (Figures 1K and S2M). Levels of *Ins1* and *Ins2* and *Gcg* and *Iapp* were indistinguishable from that of control mice both on NC (Figure 1K) and HF (Figure S2M) diets. Neither the mRNA levels for enzymes involved in glucose metabolism (*Gck*, *Pklr*, and *G6pc2*) nor receptors for insulin release and glucose sensing (*Insr*, *Gipr*, *Glp1r*, and *Slc2a2*) were affected by depletion of TCF4. Moreover, the expression of β cell transcription factors (*Pdx1*, *NeuroD1*, *Nkx2.2*, *Nkx6.1*, *Isl1*, and *FoxO1*) was not affected in isolated pancreatic islets of βTCF4KO mice (both on NC [Figure 1K] and HF [Figure S2M] diets). Of interest, *Axin2* and *Sp5*, two generic Wnt target genes (Lustig et al., 2002; Weidinger et al., 2005), showed no change both on NC (Figure 1K) and HF (Figure S2M) diets, implying that TCF4-dependent Wnt signaling is not operative in pancreatic β cells.

Tcf7l2$^{-/-}$ Newborns Die Because of Hypoglycemia

The lack of a metabolic phenotype of the βTCF4KO mice prompted us to reassess the *Tcf7l2*$^{-/-}$ model. *Tcf7l2*$^{-/-}$ newborns appeared developmentally normal at birth yet displayed a reduced body weight (Figure 2A). They became lethargic within hours after birth, presumably because of lack of energy to compete for nourishment, and typically died after 8 hr (Figure 2D). Just after birth, glucose levels appeared indistinguishable between *Tcf7l2*$^{+/+}$, *Tcf7l2*$^{+/-}$, and *Tcf7l2*$^{-/-}$ newborns (data not shown). However, glucose levels were significantly lower at 3 hr postpartum (hpp) in the *Tcf7l2*$^{-/-}$ newborns (Figure 2B) than in littermates. The hypoglycemia was caused neither by glycosuria (data not shown) nor by excessive insulin secretion, as plasma insulin levels were also significantly lower in *Tcf7l2*$^{-/-}$ mice than in their *Tcf7l2*$^{+/+}$ and *Tcf7l2*$^{+/-}$ littermates (Figure 2C). The *Tcf7l2*$^{-/-}$ newborns could be rescued for up to 32 hr by subcutaneous injections of 50 μl of 10% glucose at birth and every 6 hr thereafter ($p < 0.001$) (Figure 2D).

Hepatic Glucose Metabolism Is Affected in *Tcf7l2*$^{-/-}$ Newborns

To circumvent confounding consequences of feeding, we removed all pups from the mothers directly after birth and analyzed metabolic parameters 5 hr later (5 hpp). To ensure survival of the newborns, all mice were given a single subcutaneous glucose injection at birth. Blood glucose levels and plasma insulin levels were indistinguishable between 5 hpp *Tcf7l2*$^{+/+}$, *Tcf7l2*$^{+/-}$, and *Tcf7l2*$^{-/-}$ (Figures 3A and 3B) newborns. This was in line with the previous results obtained in adult mice, where the absence of TCF4 did not prevent β cells

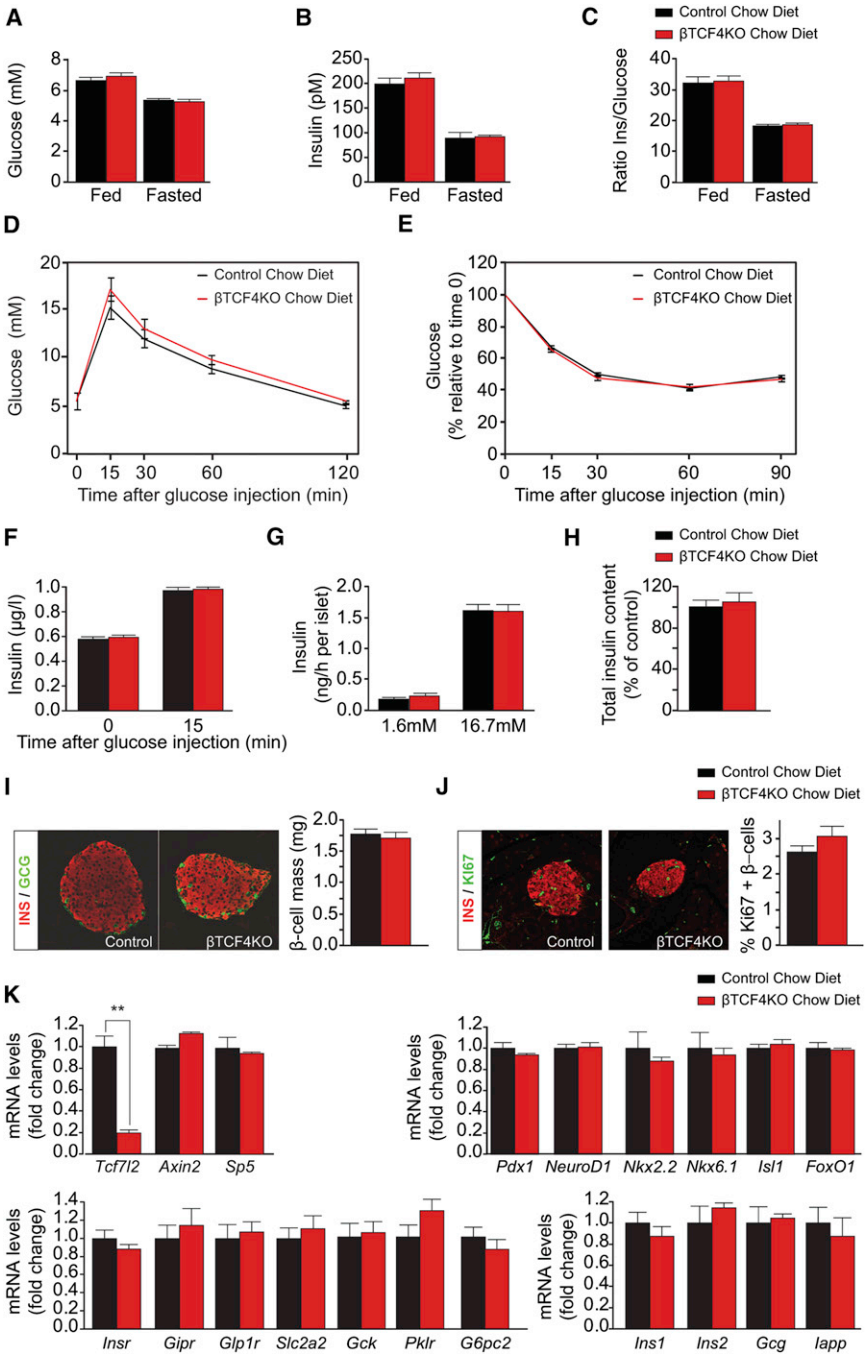

Figure 1. β-Cell-Specific Deletion of *Tcf7l2* Does Not Affect Islet Architecture and Pancreatic β Cell Function In Vivo and In Vitro

(A–C) (A) Blood glucose, (B) plasma insulin, and (C) ratio insulin versus glucose levels in fed state (Fed) and after a 16 hr fasting (Fasted) in control (*Tcf7l2* $^{loxp/loxp}$) and βTCF4KO (*Tcf7l2* $^{loxp/loxp}$;*RIP-Cre-ER*^{T2}) littermates at the age of 12 weeks.

(D and E) (D) GTT and (E) ITT were performed in βTCF4KO and control mice after 16 hr and 4 hr fasting, respectively.

(F) After 16 hr of fasting, plasma insulin levels were measured at time 0 and 15 min after glucose injection to test insulin secretion in vivo in βTCF4KO and control mice.

(G) Insulin release did not differ between control and βTCF4KO isolated pancreatic islets at 1.6 mM and 16.7 mM glucose.

(H) Total insulin content also did not differ between control and βTCF4KO pancreatic islets.

(I) Pancreatic islets from control and βTCF4KO adult mice. Sections were stained with anti-insulin (red) and anti-glucagon (green) antibodies. β cell mass did not differ between control and βTCF4KO mice, n = 4 per genotype.

(J) Pancreatic islets from control and βTCF4KO adult mice stained with anti-KI67 (green) and anti-insulin (red) antibodies, n = 4 per genotype.

(K) qRT-PCR to measure relative *Tcf7l2* and the Wnt target genes as well as the mRNA levels of relevant genes for β cell function in isolated pancreatic islets from control and βTCF4KO mice, n = 8 per genotype.

All data are represented as mean ±SEM; n = 12–15 per genotype; **p < 0.01. See also Figures S1 and S2.

from secreting insulin after glucose stimulation. Indeed, embryonic development of the endocrine pancreas, β cell proliferation, and expression of relevant β cell genes appeared normal in *Tcf7l2*$^{-/-}$ newborns (Figures S3A–S3C).

The liver occupies a central position in metabolic adaptation after birth, particularly in glucose homeostasis. Initially, hepatic glucose is released from glycogen stores. After several hours of fasting, gluconeogenesis, the production of glucose from lactate and pyruvate, becomes the major source of glucose (Gustafsson, 2009; Pilkis and Granner, 1992). We analyzed periodic acid Schiff (PAS) staining for glycogen at late stages of embryonic development and after birth. At E18.5, *Tcf7l2*$^{-/-}$ and WT livers had accumulated similar levels of glycogen (Figure 3C, top), implying that glycogen metabolism is not affected by TCF4 during embryonic development. In contrast, histological sections and measurement of glycogen content of liver samples from 5 hpp *Tcf7l2*$^{-/-}$ mice revealed strongly reduced glycogen storage (p < 0.01) (Figure 3C, bottom, and Figure 3D).

mRNA expression levels of enzymes important for glycogen metabolism (*Gys2*, *Pygl*, and *Gyg*) and gluconeogenesis (*Pck1*, *G6pc*, and *Fbp1*) were analyzed by qRT-PCR in embryonic and 5 hpp *Tcf7l2*$^{-/-}$ and WT livers. Expression of *Gys2*, the enzyme that catalyzes the rate-limiting step in the synthesis of glycogen (Ferrer et al., 2003), was significantly downregulated in 5 hpp *Tcf7l2*$^{-/-}$ livers (p < 0.05) (Figure 3E). Consistent with an activation of the gluconeogenic pathway at birth, *Pck1*, *G6pc*, and *Fbp1* mRNA levels were upregulated in the WT newborn livers compared with the embryonic livers. The induction of *Pck1* and

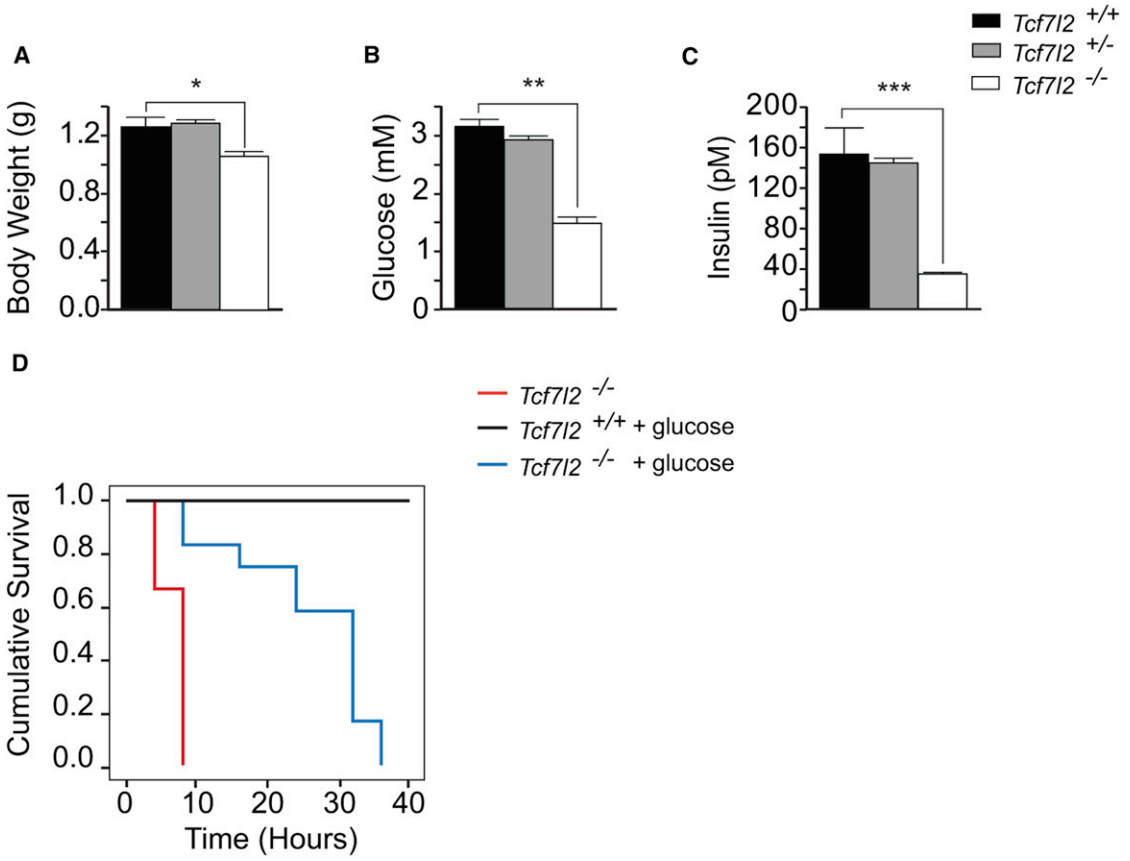

Figure 2. *Tcf7l2*$^{-/-}$ Newborns Succumb to Acute Hypoglycemia

(A–C) (A) Body weight, (B) blood glucose, and (C) plasma insulin levels in 3 hpp *Tcf7l2*$^{+/+}$, *Tcf7l2*$^{+/-}$, and *Tcf7l2*$^{-/-}$ newborns.

(D) After subcutaneous administration of glucose at birth and every 6 hr thereafter, the life span of the *Tcf7l2*$^{-/-}$ newborns can be extended significantly ($p < 0.0001$) compared with nontreated *Tcf7l2*$^{-/-}$ newborns.

Data are represented as mean ±SEM. *$p < 0.05$, **$p < 0.01$, and ***$p < 0.001$; n = 12–15 per genotype. See also Figure S3.

G6pc was significantly reduced in the 5 hpp *Tcf7l2*$^{-/-}$ newborn livers when compared with WT littermates ($p < 0.05$) (Figure 3F).

Tcf7l2$^{-/-}$ Newborns Have Disrupted Hepatic Lipid Metabolism

After birth, triglyceride synthesis, fatty acid oxidation, and ketone body synthesis are also enhanced in the early postnatal liver (Ferré et al., 1986). To determine the effect of TCF4 depletion on lipid metabolism, concentrations of free fatty acids (FFA), triglycerides, and ketone bodies were measured in the serum of 5 hpp *Tcf7l2*$^{+/+}$, *Tcf7l2*$^{+/-}$, and *Tcf7l2*$^{-/-}$ newborns, previously removed from their mothers and injected with glucose at birth. Serum FFA, triglycerides, and ketone bodies levels were significantly reduced in 5 hpp *Tcf7l2*$^{-/-}$ newborns ($p < 0.01$ and $p < 0.05$) (Figures 4A–4C). We then assessed hepatic lipid distribution with oil red O staining. Embryonic livers from WT and *Tcf7l2*$^{-/-}$ mice were indistinguishable, presenting few small lipid droplets (Figure 4D, top). However, 5 hpp WT livers showed a strong increase in lipid, which was not observed in *Tcf7l2*$^{-/-}$ livers (Figure 4D, bottom). In concordance, triglyceride content was significantly reduced in 5 hpp *Tcf7l2*$^{-/-}$ livers when compared with *Tcf7l2*$^{+/+}$ and *Tcf7l2*$^{+/-}$ ($p < 0.01$) (Figure 4E).

Changes in serum and hepatic lipid levels were possibly secondary to changes in gene expression of relevant enzymes in hepatic lipid metabolism. Indeed, the upregulation of genes involved in different aspects of fatty acid biosynthesis observed in 5 hhp WT livers was again abolished in 5 hpp *Tcf7l2*$^{-/-}$ livers. This included *Acadl* and *Ehhadh* ($p < 0.05$ and $p < 0.01$) (Figure 4F). Similarly, decreases were detected in the expression of several enzymes involved in β-oxidation, such as *Acaa1a* and *Acot4* ($p < 0.05$ and $p < 0.01$) (Figure 4G), and genes implied in ketogenesis and cholesterol metabolism, such as *Fgf21*, *Akr1c6*, and *Cyp7a1* ($p < 0.05$) (Figure 4H).

Strong Upregulation of Wnt, Liver-Zonated, and Metabolic Genes in Postnatal Livers in a TCF4-Dependent Manner

The failed postnatal upregulation of multiple metabolic genes prompted us to address the possibility that these genes are regulated by the Wnt pathway effector TCF4. To identify the hepatic transcriptional signature dependent on TCF4, we performed comparative gene expression profiling on livers of 5 hpp newborns. 960 genes were differentially expressed between *Tcf7l2*$^{-/-}$ and *Tcf7l2*$^{+/+}$ livers (as arbitrarily defined by >2-fold

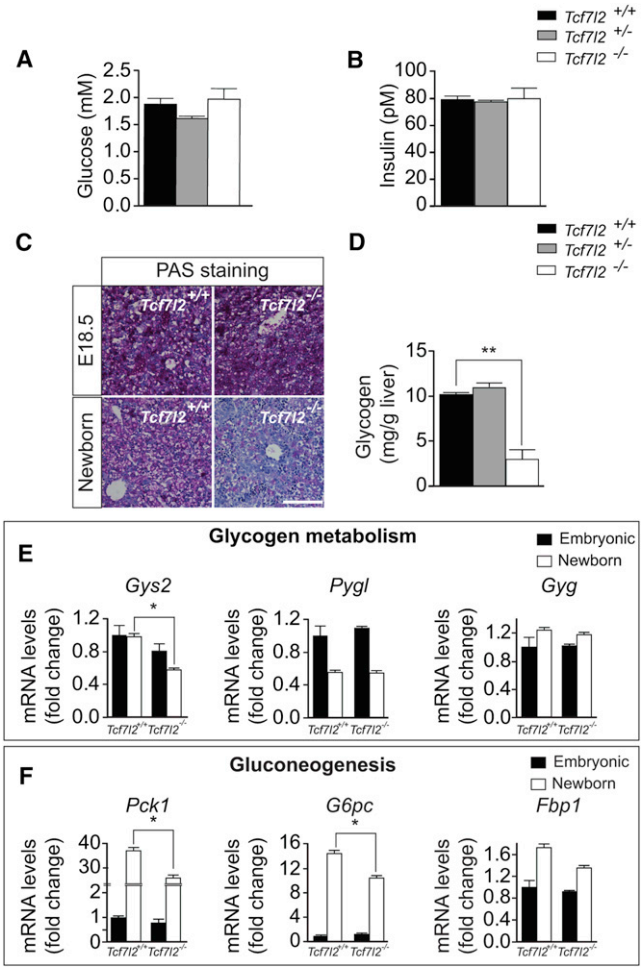

Figure 3. *Tcf7l2* Deficiency Results in Impaired Carbohydrate Metabolism in the Newborn Liver

(A and B) (A) Blood glucose and (B) plasma insulin levels were measured in $Tcf7l2^{+/+}$, $Tcf7l2^{+/-}$, and $Tcf7l2^{-/-}$ 5 hpp newborns.

(C) PAS staining for glycogen (magenta) in livers from day 18.5 $Tcf7l2^{+/+}$ and $Tcf7l2^{-/-}$ fetuses (top) and 5 hpp $Tcf7l2^{+/+}$ and $Tcf7l2^{-/-}$ newborns (bottom). Scale bar, 100 μm.

(D) Glycogen levels were measured in $Tcf7l2^{+/+}$, $Tcf7l2^{+/-}$, and $Tcf7l2^{-/-}$ livers from 5 hpp newborns.

(E and F) (E) qPCR to measure relative mRNA levels of genes involved in glycogen metabolism and (F) gluconeogenesis, from either embryonic or 5 hpp $Tcf7l2^{+/+}$ and $Tcf7l2^{-/-}$ livers. All qRT-PCR results were normalized to housekeeping mRNA levels and were expressed relative to $Tcf7l2^{+/+}$ embryonic samples.

All data are represented as mean ±SEM; n = 6–12 per genotype; *p < 0.05 and **p < 0.01.

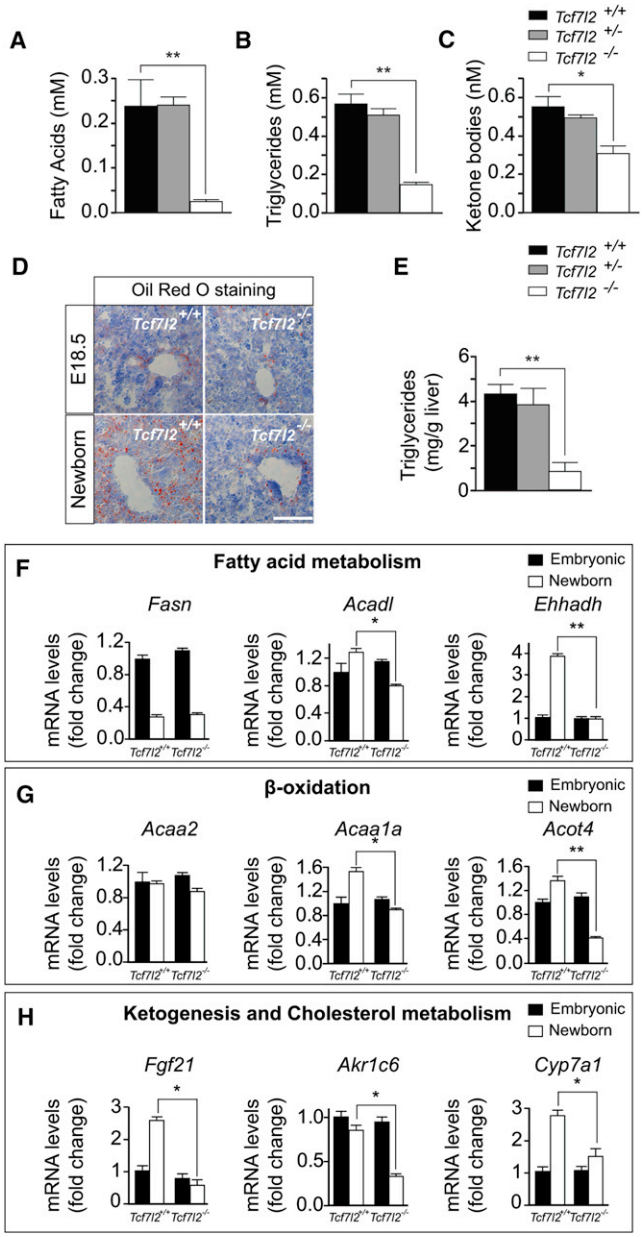

Figure 4. *Tcf7l2* Deficiency Results in Impaired Lipid Metabolism in the Newborn Liver

(A–C) (A) Serum fatty acids, (B) triglycerides, and (C) ketone bodies levels were measured in $Tcf7l2^{+/+}$, $Tcf7l2^{+/-}$, and $Tcf7l2^{-/-}$ 5 hpp newborns.

(D) Oil red O staining for lipid droplets (red) in livers from day 18.5 $Tcf7l2^{+/+}$ and $Tcf7l2^{-/-}$ fetuses (top) and 5 hpp $Tcf7l2^{+/+}$ and $Tcf7l2^{-/-}$ newborns (bottom). Scale bar, 100 μm.

(E) Triglyceride levels were measured in $Tcf7l2^{+/+}$, $Tcf7l2^{+/-}$, and $Tcf7l2^{-/-}$ livers from 5 hpp newborns.

(F–H) (F) qPCR to measure relative mRNA levels of genes involved in fatty acid metabolism, (G) β-oxidation, and (H) ketogenesis and cholesterol metabolism from either embryonic or 5 hpp $Tcf7l2^{+/+}$ and $Tcf7l2^{-/-}$ livers. All qRT-PCR results were normalized to housekeeping mRNA levels and are expressed relative to $Tcf7l2^{+/+}$ embryonic samples.

All data are represented as mean ±SEM; n = 6–12 per genotype; *p < 0.05 and **p < 0.01.

expression difference; p < 0.05) (Table S1 and Figure 5A). In the list of genes with lower expression in the mutant mice, we found metabolic genes such as *Aqp9*, *Slc17a2*, and *Akr1c6*. We also noted differential expression levels of the generic Wnt target genes *Axin2* and *Sp5* between $Tcf7l2^{-/-}$ and $Tcf7l2^{+/+}$ neonatal livers (Figure 5D). A previous report has implicated Wnt signaling in the zonation of genes in adult liver and has identified several liver-specific Wnt/β-catenin target genes such as *Glul* and

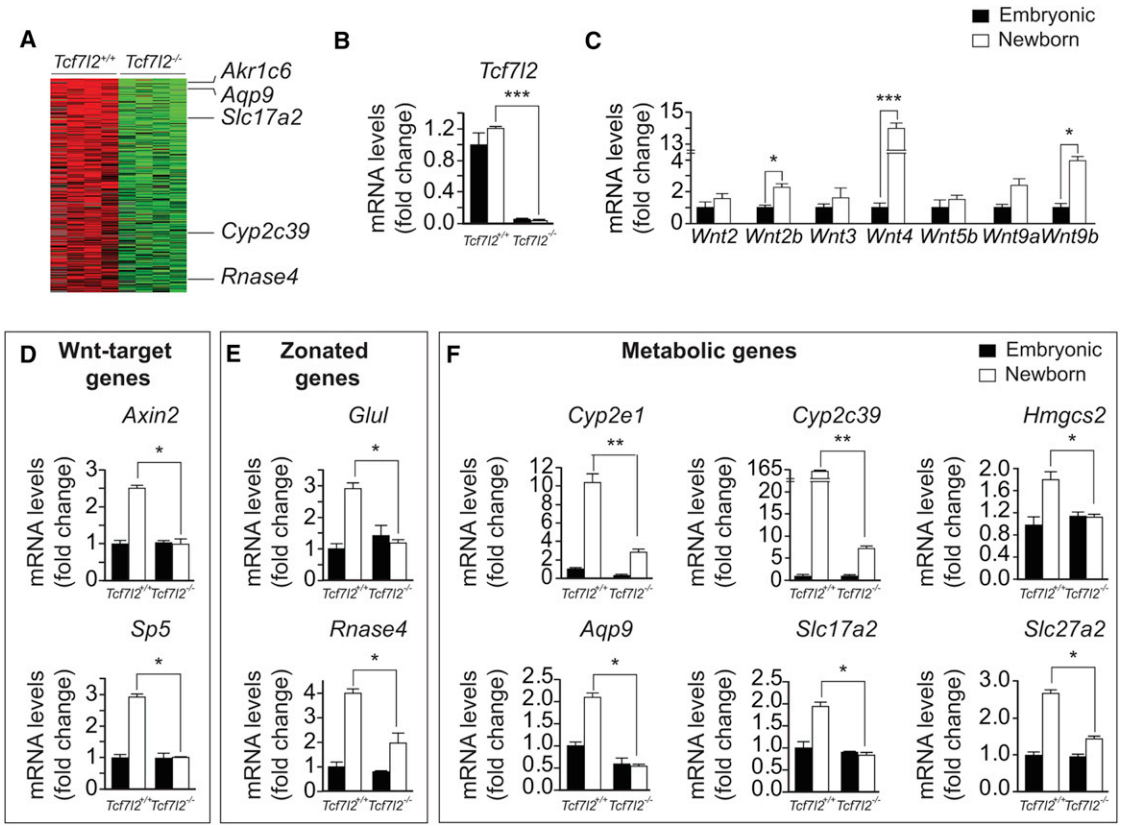

Figure 5. Wnt-Dependent, Liver-Zonated, and Metabolic Genes Are Upregulated in Liver after Birth in a TCF4-Dependent Manner

(A) Heatmap showing genes downregulated more than 2-fold with $p < 0.05$ after mean centering in *Tcf7l2*$^{-/-}$ versus *Tcf7l2*$^{+/+}$ newborn livers. Red, upregulated; green, downregulated; black, no change; gray, missing data. Representatives of TCF4 metabolic target genes are listed on the right.

(B–F) (B) qRT-PCR to measure relative *Tcf7l2*, (C) Wnt genes, (D) Wnt target genes, (E) liver-zonated genes, and (F) metabolic gene mRNA levels in embryonic and 5 hpp liver samples from *Tcf7l2*$^{+/+}$ and *Tcf7l2*$^{-/-}$ mice, respectively. All qRT-PCR results were normalized to housekeeping mRNA levels and are expressed relative to *Tcf7l2*$^{+/+}$ embryonic samples.

Data are represented as mean ±SEM; n = 8 per genotype; *$p < 0.05$, **$p < 0.01$, and ***$p < 0.001$. See also Figure S4 and Table S1.

Rnase4 (Benhamouche et al., 2006). These Wnt-driven zonation genes were also differentially expressed between *Tcf7l2*$^{-/-}$ and *Tcf7l2*$^{+/+}$ neonatal livers (Figure 5E). These observations implied that Wnt signals, mediated through TCF4, are operative in the early postnatal liver.

Given that the metabolic phenotypes were observed in *Tcf7l2*$^{-/-}$ postnatal livers, but not during embryonic development, we hypothesized that TCF4 transcriptional target gene expression may follow the same pattern. As expected, there were no significant differences in the mRNA levels of the two prototypic Wnt-responsive genes *Axin2* and *Sp5* in *Tcf7l2*$^{-/-}$ embryonic livers when compared with WT littermates (Figure 5D). When we compared mRNA levels between late embryonic and 5 hpp WT livers, we noted a dramatic upregulation of these generic Wnt target genes (Figure 5D), implying that the Wnt pathway is acutely activated directly after birth. This induction did not occur in the *Tcf7l2*$^{-/-}$ newborn livers ($p < 0.05$) (Figure 5D). Indeed, we observed an increase in the expression levels of several *Wnt* genes in postnatal livers when compared with their embryonic levels ($p < 0.05$ and $p < 0.01$) (Figure 5C). There was also a significant upregulation after birth of the liver-zonated Wnt-target genes *Glul* and *Rnase4*, again in a TCF4-dependent manner ($p < 0.05$) (Figure 5E). Of note, *Tcf7l2* mRNA levels were not increased after birth (Figure 5B).

As noted above, the microarray list of genes that were low in *Tcf7l2*$^{-/-}$ newborn livers compared to controls contained multiple genes relevant to the metabolic functions of the liver, such as *Aqp9*, an essential glycerol transporter (Rojek et al., 2007); *Cyp2e1*, a monooxygenase member of the cytochrome P450 superfamily that catalyzes steps in the synthesis of cholesterol, steroids, and other lipids (Lieber, 1997); and *Hmgcs2*, the rate-limiting enzyme in the ketogenesis pathway, providing lipid-derived energy in neonates and in times of carbohydrate deprivation (Dashti and Ontko, 1979) (Table S1). In line with the previous observations in Wnt and liver-zonated genes, metabolic genes such as *Cyp2e1*, *Cyp2c39*, *Hmgcs2*, *Aqp9*, *Slc17a2*, and *Slc27a2* were significantly upregulated postnatally in WT livers, but such upregulation did not occur in the *Tcf7l2*$^{-/-}$ postnatal livers ($p < 0.05$ and $p < 0.01$) (Figure 5F). These differences were also observed between 5 hpp *Tcf7l2*$^{+/+}$ and *Tcf7l2*$^{-/-}$ livers at the protein level by immunostaining and western blot analysis for AQP9, CYP2E1, and SLC27A2 (Figures S4A and S4B).

TCF4 Directly Regulates the Expression of Key Genes Involved in Metabolic Pathways

The transcriptional signature of *Tcf7l2*$^{-/-}$ postnatal livers suggested that TCF4 might activate the expression of the pertinent metabolic genes directly. We performed chromatin immunoprecipitation sequencing (ChIP-seq) experiments on chromatin prepared from livers of 1-week-old WT mice. 5,092 potential TCF4 binding sites were identified (at a 10% false discovery rate) (Figures 6A, 6B, S5A, and S5B and Table S2). The most common sequence motif in the TCF4-binding regions closely resembled the cognate TCF-binding motif (Figure 6C and Table S3) (Hatzis et al., 2008; van de Wetering et al., 1997). GSEA analysis showed a significant enrichment of genes with TCF4 binding sites within 5 kb from their transcription start sites (TSSs) among the genes with decreased expression in newborn *Tcf7l2*$^{-/-}$ livers (Figure 6D). Thus, we identified TCF4 peaks in the TSSs of general Wnt target genes such as *Axin2* and *Sp5* (Hatzis et al., 2008), which coincided with similar peaks in intestinal crypt chromatin (Figures 6A and S5A). We also identified TCF4 peaks in the vicinity of the TSSs of the liver-zonated genes *Glul* and *Rnase4* (Figures 6A and S5A). These results were confirmed by qPCR ($p < 0.05$, $p < 0.01$, and $p < 0.001$) (Figures 6E and S5C).

We then performed Gene Ontology (GO) analysis (Eden et al., 2009) on a set of genes defined as being >1.5-fold downregulated in the *Tcf7l2*$^{-/-}$ postnatal livers and containing at least one TCF4-bound region within 5 kb from the TSS. Among the functional categories significantly enriched in this gene set ($p < 0.001$), the overwhelming majority was involved in metabolic processes, including carbohydrate, steroid, ketone, and lipid metabolism (Table S4). Among these key liver metabolic genes identified as novel TCF4 target genes, we noted, among others, *Aqp9*, *Acadl*, *Akr1c6*, *Cyp2e1*, *Cyp2c39*, *Slc25a21*, and *Hmgcs2*a (Figures 6B, 6E, S5B, and S5C). As a further validation to the ChIP-seq data, we cloned the *Sp5*, *Rnase4*, *Cyp2e1*, and *Akr1c6* promoters and the putative *Aqp9* enhancer in a luciferase reporter plasmid. Transient transfections were performed in HepG2 cells, a human hepatocarcinoma cell line in which Wnt signaling is constitutively active due to a β-catenin mutation (de La Coste et al., 1998). Figure 6F shows spontaneous activity of the β-catenin/TCF reporter plasmid TOPflash (Korinek et al., 1997) and of all putative regulatory sequences due to the activation of Wnt signaling in this cell line. As a negative control, we used the mutant FOP reporter plasmid (Figure 6F). In order to demonstrate that the measured transcriptional activity was dependent on TCF4, all constructs were cotransfected with a TCF4 dominant-negative (ΔNTCF4) expression plasmid (Hatzis et al., 2008; van de Wetering et al., 2002). As expected, luciferase activity was significantly reduced upon ΔNTCF4 overexpression (and consequent reduction of WT TCF4 activity) ($p < 0.05$ and $p < 0.01$) (Figure 6G), corroborating that this set of metabolic genes is regulated directly by TCF4.

In Adult Liver, TCF4 Is Involved in the Transcriptional Activation of Genes Implicated in the Response to Fasting

As TCF4 is a critical regulator of neonatal hepatic metabolism in vivo and as a loss of TCF4 leads to lethal hypoglycemia in newborn mice, we investigated whether depletion of TCF4 in adult liver would alter glucose homeostasis. For the generation of liver-specific TCF4 knockout mice (LTCF4KO), we followed the same strategy that we have described previously for generating βTCF4KO mice but instead bred *Tcf7l2*^{loxP} mice with the tamoxifen-inducible liver-specific Cre recombinase strain *SA-Cre-ER*^{T2} (Schuler et al., 2004). In all experiments, *Tcf7l2*$^{loxp/loxp}$; *SA-Cre-ER*^{T2} (LTCF4KO) and *Tcf7l2*$^{loxp/loxp}$ control mice were injected with tamoxifen after weaning and were analyzed at the age of 2 to 3 months.

To determine the efficiency of recombination of the *Tcf7l2* gene in the liver, genomic PCR and real-time PCR were performed. As shown in Figure S6A, recombination took place specifically in DNA samples from LTCF4KO livers. In concordance, expression of *Tcf7l2* mRNA was strongly reduced in the livers from LTCF4KO mice when compared with control mice (Figure S6B). LTCF4KO mice did not differ in body weight from their control littermates on NC diet (Figure S6D). However, we observed significantly reduced glucose levels in fasting LTCF4KO mice when compared to control mice (Figure S6G). This reduced glucose level was not caused by hyperinsulinemia (Figures S6H and S6I). Indeed, glucose-stimulated insulin secretion did not differ between LTCF4KO and control mice on NC diet (Figure S6M).

Based on the fact that newborn *Tcf7l2*$^{-/-}$ and adult LTCF4KO showed decreased blood glucose levels upon fasting, we assessed the hepatic response to long-term fasting in LTCF4KO mice. Blood glucose measurements were taken from LTCF4KO mice along with control littermates at regular intervals during a 24 hr fasting period. We found significantly reduced blood glucose levels between LTCF4KO and control mice from 9 hr onward during the 24 hr fasting period ($p < 0.05$) (Figure 7A). No differences in blood glucose levels were observed in mice fed ad libitum with NC diet (Figures 7A and S6G). To explore the possible mechanism underlying the reduced glucose levels observed in LTCF4KO mice during long fasting periods, we compared microarray data from livers of control mice in fed and 24-hr-fasted states in order to identify the genes upregulated in response to fasting. 623 genes were differentially expressed between fed and 24-hr-fasted control livers (as defined by being >2-fold upregulated; $p < 0.05$) (Table S5 and Figure 7B). The induction of this set of genes upon fasting was generally much less prominent in LTCF4KO samples (Table S5 and Figure 7B). GSEA analysis showed a significant enrichment of genes with at least one TCF4 peak within 5 kb from the TSS among the genes differentially expressed between LTCF4KO versus control livers fasted during 24 hr (24-hr-fasted $p < 0.001$ versus fed $p < 0.789$) (Figure 7C and data not shown). Furthermore, GSEA analysis showed a significant enrichment of metabolic pathways, such as glycolysis and gluconeogenesis, biosynthesis of steroids, and fatty acid metabolism in the set of genes that were lower in 24-hr-fasted LTCF4KO livers when compared with 24-hr-fasted control livers (Table S6). In contrast, GSEA did not find any metabolic category significantly enriched when fed LTCF4KO livers were compared with fed control livers (data not shown).

Between fed and 24-hr-fasted control livers, we noted an upregulation of the generic Wnt targets genes *Axin2* and *Sp5* (Figure S7H), implying that the Wnt pathway is activated upon

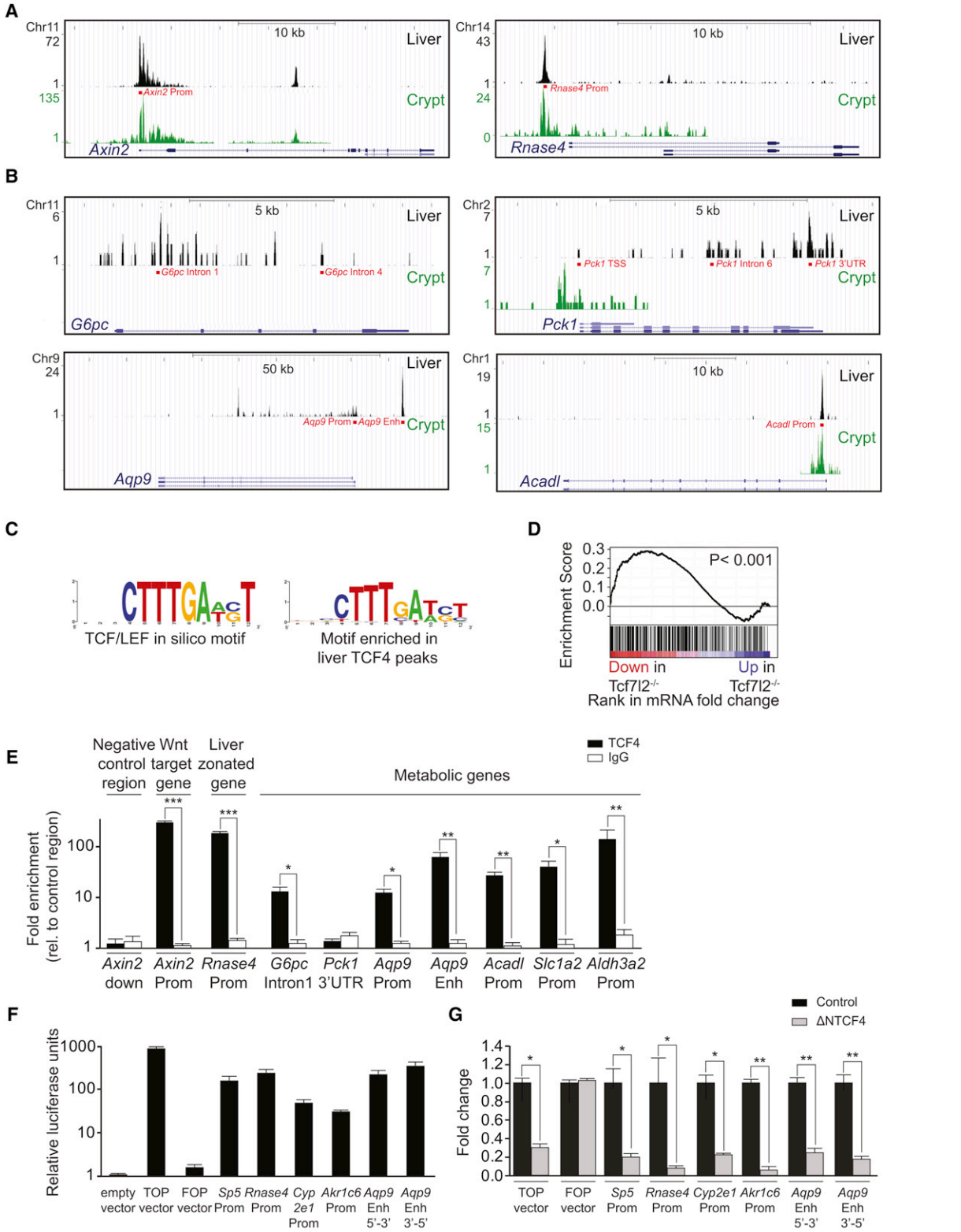

Figure 6. Enrichment of TCF4 Binding in the Vicinity of Metabolic Genes Expressed in Newborn Liver

(A and B) Schematic representation of (A) *Axin2* and *Rnase4* and (B) *G6pc*, *Pck1*, *Aqp9*, and *Acadl* loci, indicating the location of ChIP-seq TCF4 peaks in mouse intestinal crypt and liver chromatin. Location of the PCR products detected by qPCR to confirm the ChIP-seq results are indicated in red.

(C) Sequence logos illustrating the TCF/LEF in silico motif and the most enriched motif in the TCF4 ChIP-seq peaks in chromatin from liver.

(legend continued on next page)

fasting. This induction did not occur in the LTCF4KO livers (Figure S7H). The liver-zonated Wnt/β-catenin target genes *Glul* and *Rnase4* were also significantly upregulated during fasting in a TCF4-dependent fashion (Figure S7H). This implied that TCF4 is involved in a Wnt-driven transcriptional response to fasting. In agreement, fasting increased *Wnt2b*, *Wnt4*, and *Wnt9b* expression in control liver (Figure S6C). We also examined the hepatic mRNA levels of known genes involved in fasting such as *Aldh3a2*, *St3gal5* (Sanderson et al., 2009), and *Slc1a2* (Table S5 and Figure 7D). Expression was upregulated after 24 hr of fasting, and their induction was abolished by TCF4 ablation ($p < 0.01$) (Figure 7D). Additionally, the fasting-mediated mRNA induction of one of the key gluconeogenic enzymes, *G6pc*, was significantly reduced in LTCF4KO liver samples ($p < 0.05$) (Figure 7D). Importantly, analysis of the ChIP-seq data and qPCR demonstrated the presence of TCF4 peaks in near metabolic genes involved in the response to fasting such as *G6pc*, *Aldh3a2*, and *Slc1a2* (Figures 6B, 6E, S5B, and S5C). Of note, TCF4 was not significantly enriched in the vicinity of *Pck1*, *Fbp1*, and *St3gal5* genes (Figures 6B, 6E, S5B, and S5C).

LTCF4KO Mice Display Reduced Hepatic Gluconeogenesis

To assess the effect of liver-specific TCF4 depletion on whole-body glucose utilization, LTCF4KO and control mice were fed with either NC or HF diet. We observed no significant differences in body weight, gain of weight, and food intake between LTCF4KO and control mice on HF diet during an 8 week period (Figures S6D–S6F). However, we observed significantly reduced glucose levels in fasting LTCF4KO mice when compared to control mice ($p < 0.05$) (Figure S6J). This reduced glucose level was not caused by hyperinsulinemia (Figures S6K and S6L). Indeed, glucose-stimulated insulin secretion did not differ between LTCF4KO and control mice (Figure S6N) on HF diet.

Intraperitoneal GTT were performed on LTCF4KO and control mice maintained on both diets. Although we observed a mild phenotype in LTCF4KO mice fed with NC diet (Figure S7A), upon challenge with HF diet, the mice exhibited a significantly lower increase in glucose levels ($p < 0.05$) (Figure S7B). Following injection of pyruvate, we also observed that glucose levels were lower in LTCF4KO mice on NC diet (Figure 7E) and became significantly less increased in LTCF4KO upon challenge with HF diet ($p < 0.05$) (Figure 7F). Collectively, these results indicated that LTCF4KO mice have a reduced hepatic gluconeogenesis that becomes more pronounced when mice are challenged with HF diet. To directly examine the effect of TCF4 deficiency on hepatic glucose production in vitro, hepatocytes from control and LTCF4KO mice on HF diet were isolated and assayed in culture. TCF4 null hepatocytes secreted less glucose than controls following either glucagon or IBMX (3-isobutyl-1-methylxanthine) stimulation, indicating an intrinsic impairment of glucose production (Figure S7C). The induction of TCF4-dependent *G6pc* and *Aldh3a2* mRNA levels in response to glucagon stimulation, as a surrogate of fasting, was significantly abrogated in LTCF4KO hepatocytes ($p < 0.05$) (Figure S7D).

Effects of Liver-Specific Overexpression of TCF4 In Vivo Opposite to LTCF4KO

Adult liver-specific *Tcf7l2* knockout mice (LTCF4KO) showed reduced blood glucose levels and hepatic glucose production. To determine whether overexpression of TCF4 specifically in the liver induces the opposite phenotype, we analyzed the metabolic effects after transient hepatic overexpression of TCF4 by using replication-deficient adenovirus administered by tail vein injection into adult mice (Fechner et al., 1999). In mice injected with TCF4 adenovirus (Ad-TCF4), ~50% of the nuclei displayed increased expression of TCF4 (Figure 7G, right, white arrowheads). Ad-TCF4-injected mice displayed a significant increase in serum glucose under fasting conditions (Figure S7E) compared to controls. This difference was not due to a reduction in circulating insulin concentrations (Figures S7F and S7G). Consistent with our observation after liver-specific deletion of TCF4, overexpression of TCF4 specifically in the liver led to an increased hepatic glucose production upon pyruvate injection (Figure 7H).

qPCR analyses revealed an upregulation of the generic Wnt target genes (*Axin2* and *Sp5*) and liver-zonated genes (*Glul* and *Rnase4*) ($p < 0.05$) (Figure S7I), implying that elevating TCF4 indeed enhances the transcriptional Wnt response. This induction also occurred for the metabolic genes that were direct targets of TCF4 (*Aldh3a2*, *St3gal5*, *Slc1a2*, and *G6pc*) ($p < 0.05$) (Figure 7I). Of note, metabolic genes that were not TCF4 targets (*Pck1* and *Fbp1*) were not upregulated after TCF4 overexpression (Figure 7I). Thus, in the adult liver, genetic overexpression of TCF4 leads to the opposite effect of removal of TCF4 in terms of glucose metabolism and of expression of the Wnt-responsive metabolic genes.

DISCUSSION

Most studies on the involvement of *TCF7L2* SNP variants in type 2 diabetes (T2D) focus on a role of TCF4 in pancreatic islets and β cells (da Silva Xavier et al., 2009; Lyssenko et al., 2007; Shu et al., 2008, 2009). In this study, we utilize mouse genetics to show that removal of TCF4 from β cells does not affect their function. These observations are made in newborn *Tcf7l2*$^{-/-}$ mice and in adult β-cell-specific *Tcf7l2* mutants, challenged by fasting or by high-fat diet. The previously reported changes in β cell function possibly result indirectly from changes elsewhere in the body. In this study, we have focused on the transcriptional role of TCF4 in liver metabolism. We believe it highly likely that

(D) GSEA showing a significant enrichment of genes bound by TCF4 among the genes downregulated in *Tcf7l2*$^{-/-}$ newborn livers.
(E) qPCR was performed to determine enrichment of TCF4 and IgG control in the proximal promoters and enhancers of several TCF4 target genes.
(F) Luciferase units relative to the activity detected of the respective empty vector.
(G) Same constructs described above were cotransfected with control or ΔNTCF4 (dominant-negative TCF4) plasmid. Values were normalized to the luciferase activity of the respective empty vector.
Data are represented as mean ±SEM from three independent experiments. *$p < 0.05$, **$p < 0.01$, and ***$p < 0.001$. See also Figure S5 and Tables S2, S3, and S4.

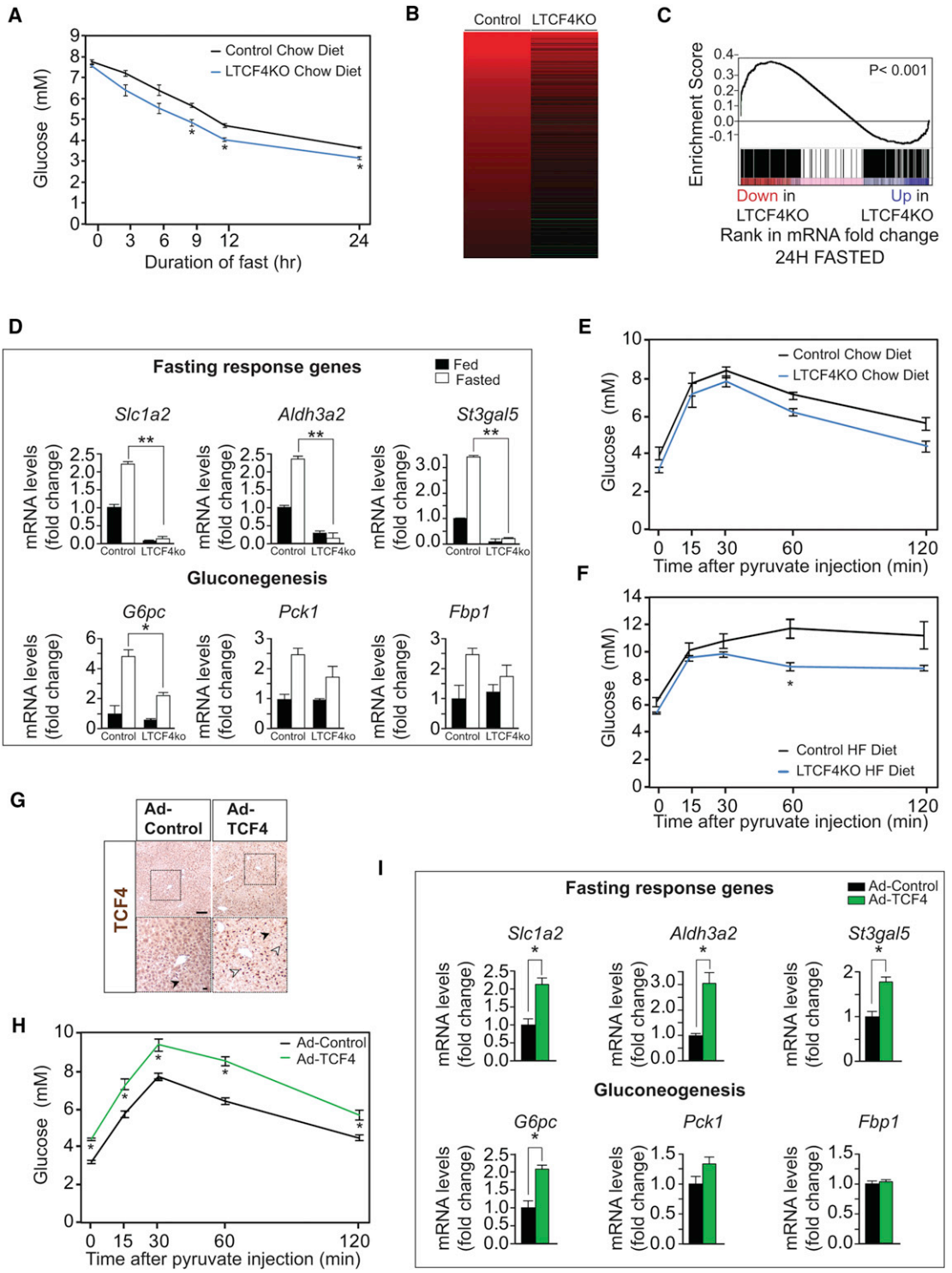

Figure 7. Modulation of TCF4 Levels in the Liver Affects Hepatic Glucose Production

(A) Blood glucose levels of control and LTCF4KO mice during the course of a 24 hr fast.

(B) Heatmap showing genes upregulated more than 2-fold with $p < 0.05$ in 24-hr-fasted versus fed comparison in control and the comparison of the corresponding upregulation in LTCF4KO adult livers. Red, upregulated; green, downregulated; black, no change; gray, missing data.

(C) GSEA showing significant enrichment of genes bound by TCF4 among the genes downregulated in LTCF4KO adult livers in 24-hr-fasted state.

(D) qRT-PCR to measure relative mRNA levels of metabolic genes involved in the response to fasting and gluconeogenesis. All qRT-PCR results were normalized to housekeeping mRNA levels and are expressed relative to control fed samples.

(legend continued on next page)

a Wnt/TCF4 axis may similarly control transcriptional responses to metabolic challenge in, for instance, muscle or white adipose tissue.

The Wnt pathway controls postnatal hepatic growth (Apte et al., 2007) and postnatal liver zonation (Spear et al., 2006). We now show that TCF4 controls physiological energy-related functions of the neonatal and adult liver and that Wnt target genes are activated in response to metabolic demand in a TCF4-dependent manner. We thus identify a liver-specific TCF4-controlled gene program. Importantly, this liver-specific set of TCF4 target genes includes some generic Wnt target genes, but it otherwise mainly covers pathways related to metabolism, such as gluconeogenesis, transport of fatty acids, and synthesis of ketone bodies.

The current observations imply the following scenario. TCF4 is dispensable during embryonic development, likely due to redundancy with other TCF/LEF family members (Gregorieff et al., 2004). Moreover, it is not required for the baseline expression of its metabolic target genes throughout life, yet its function in metabolic control becomes evident under situations of metabolic demand. Its first essential role is revealed directly after birth. The immediate postnatal surge in the production of energy carriers by the liver (when placenta function is acutely disrupted) does not occur in TCF4 mutant mice, leading to their rapid death. Indeed, a large set of key metabolic liver genes are dependent on TCF4 for their induced expression after birth. We find that many of these genes are physically occupied by TCF4. Several generic Wnt target genes (*Axin2* and *Sp5*), as well as Wnt target liver-zonated genes (*Glul* and *Rnase4*), are coregulated with the set of metabolic TCF4 target genes. Several Wnt ligands are induced perinatally. This metabolic function of TCF4 is conserved into adulthood. Similar to our observations in *Tcf7l2* mutant newborns, fasting adult mice carrying a liver-specific *Tcf7l2* null mutation fail to induce generic Wnt target genes and metabolic genes involved in hepatic glucose production. As in the neonate, fasting induces several Wnt ligands. Taken together, Wnt signals activate the "surges" in liver metabolism that occur in the immediate postnatal period and upon metabolic demand in the adult.

In accordance with this, a recent study has used a transgenic mouse approach to demonstrate that the diabetes-associated SNP variants of the *TCF7L2* locus give rise to gain-of-expression alleles (Savic et al., 2011). Our adenovirus experiment demonstrates that increased liver-specific expression of TCF4 leads to increased glucose production. Indeed, an increase in fasting hepatic glucose production has been observed in human carriers of *TCF7L2* risk alleles (Lyssenko et al., 2007; Pilgaard et al., 2009). These observations may provide a molecular framework from which to understand the role of *TCF7L2*/TCF4 in the development of diabetes.

EXPERIMENTAL PROCEDURES

Animals

All different mouse models generated and analyzed are described extensively in the Supplemental Information.

Glucose and Insulin Tolerance, Insulin Secretion, Pyruvate Challenge, and Long-Term Fasting Tests

For glucose (GTT) and pyruvate (PTT) tolerance tests, mice were deprived of food for 16 hr and were injected i.p. with either glucose or pyruvate (2 g/kg body weight). Glucose from tail vein blood was then measured at time 0, 15, 30, 60, and 120 min. For insulin tolerance test (ITT), mice were deprived of food for 4 hr and were injected i.p. with insulin (0.75 units/body weight). Glucose from tail vein was then measured at time 0, 15, 30, 60, and 90 min. For glucose-stimulated insulin secretion test, mice were deprived of food for 16 hr and injected i.p. with glucose (3 g/kg body weight), and blood was collected from the tail vein at 0 and 15 min after injection. For long-term fasting experiments, blood was sampled from the tail vein of mice, which were allowed to feed ad libitum (time 0) or fasted for 3, 6, 9, 12, or 24 hr. Blood glucose concentrations were always measured with Glucometer FreeStyle (Abbott).

Serum Biochemical Measurements

Serum blood samples were collected with Microvette CB300 capillary (Sarstedt). Plasma insulin (Mercodia), free fatty acid (BioVision), triglycerides (BioAssay systems), and ketone body (BioVision) measurements were performed by ELISA.

Glycogen and Triglyceride Assays

Tissues samples from 5 hhp $Tcf7l2^{+/+}$, $Tcf7l2^{+/-}$, and $Tcf7l2^{-/-}$ newborn livers were homogenized in 6% PCA (Perchloric Acid) (200 μl/50 μg tissue). The supernatant was collected, one volume of H_2O was added, and the solution was adjusted to pH 6.5 with 10 N KOH. A fraction of each sample was incubated with five volumes of amyloglucosidase (A7420, Sigma Aldrich) (1 mg/ml in 0.2 M [pH 4.8] acetate buffer) at 40°C for 2 hr. Glucose concentrations were then determined by using the Amplex Red Glucose/Glucose Oxidase Assay Kit (Invitrogen). Samples incubated in the absence of amyloglucosidase were used as a baseline controls.

In case of measuring triglyceride levels, liver samples were homogenized in chloroform: methanol (2:1) (500 μl/50 μg tissue). 100 μl of 0.9% NaCl were added, and samples were vortexed for 2 min and centrifuged at 2,000 rpm for 5 min. Organic phase was recovered and lyophilized. Samples were resuspended in PBS-1%Triton before measurement.

Pancreatic Islet Isolation, Insulin Secretion, and Insulin Content

Pancreatic islets from βTCF4KO, LTCF4KO, and respective control mice were isolated as previously described (Párrizas et al., 2001). For secretion studies, pancreatic islets were allowed to recover for 1 day in culture in RPMI containing 11 mM glucose supplemented with 10% fetal calf serum and penicillin-streptomycin at 37°C and 5% CO_2. Equal numbers of size-matched islets were subjected to stimulation of insulin secretion at 1.6 and 16.7 mM glucose. After 1 hr of incubation in each condition, medium was collected, and insulin levels were assessed by ELISA. To measure insulin content in isolated islets,

(E and F) PTT in LTCF4KO and control mice feed during 8 weeks with either chow (D) or high-fat (E) diet.

(G) Liver sections stained with anti-TCF4 (brown) and hematoxylin (blue) in control (Ad-Control) and TCF4-overexpressing (Ad-TCF4) mice sacrificed 4 days after adenovirus injection. Magnification: 4× (left) and 10× (right). Black arrowheads indicate endogenous TCF4 levels in the hepatocytes, whereas white arrowheads indicate hepatocytes overexpressing TCF4.

(H) PTT in control and mice overexpressing human TCF4.

(I) qRT-PCR to measure relative mRNA levels of metabolic genes involved in the response to fasting and gluconeogenesis. All qRT-PCR results were normalized to housekeeping mRNA levels and were given relative to Ad-Control mice.

Data are represented as mean ±SEM; n = 10–20 per genotype (n = 6 per genotype in [H] and [I]). *$p < 0.05$ and **$p < 0.01$. See also Figures S6 and S7 and Tables S5 and S6.

pancreatic islets were sonicated in acid ethanol on ice for 15 s three times. All extracts were stored at −20°C for subsequent ELISA.

RNA Extraction, Microarray Analysis, and RT-PCR

Total RNA was obtained from embryonic, newborn, and adult liver, newborn pancreas, and adult isolated pancreatic islets and hepatocytes. RNA extraction and reverse transcription (RT) were performed as described (Párrizas et al., 2001). For expression profile comparison between 5 hpp *Tcf7l2*$^{-/-}$ and *Tcf7l2*$^{+/+}$ livers and between fed and 24-hr-fasted control and LTCF4KO livers, 1 μg of total RNA from four liver samples for each genotype, together with universal mouse reference RNA (Stratagene), were labeled by using Quick Amp Labeling Kit (Agilent Technologies) with Cy5 and Cy3, respectively. Samples were hybridized on 4x44K Whole Mouse Genome Microarrays (Agilent, G4122F) according to manufacturer's instruction. Microarray signal and background information were retrieved by using Feature Extraction (V.9.5.3., Agilent Technologies). For each pair of experiments, fluorescent signals in either channel with greater than 2-fold above the background were considered. Genes that were present in less than three out of eight arrays (four pairs of control and mutant samples for each comparison) were excluded from further analysis. Corresponding fold changes greater than 2-fold variations between average of the control and mutant samples with $p < 0.05$ (Student's t test) were considered as significant. The data were mean centered across samples for comparison in Figure 5A. The comparison between 5 hpp *Tcf7l2*$^{-/-}$ and *Tcf7l2*$^{+/+}$ livers resulted in 960 significant unique genes differentially expressed in *Tcf7l2*$^{-/-}$ postnatal liver samples (Table S1). The comparison between 24-hr-fasted versus fed adult control and LTCF4KO livers resulted in 623 unique genes significantly less upregulated in LTCF4KO samples (Table S5).

Selected candidate genes were further validated by qRT-PCR. qRT-PCR was performed on iCycler iQ Real-Time PCR Detection Systems (Bio-Rad) by using iQ SYBR Green supermix (Bio-Rad). All qRT-PCR results were normalized to *Tbp* mRNA levels. Similar results were obtained when using *Hprt* and *β-actin* to normalize. In Figures 3, 4, and 5, the WT embryonic samples were used as a reference and were compared to the mutant embryonic, WT newborn, and mutant newborn samples. In Figure 7, the fed control samples were used as a reference and were compared to the fed mutant, fasted control, and fasted mutant samples. Primer sequences are described in Table S7.

ACCESSION NUMBERS

Array data are available at Gene Expression Omnibus (http://www.ncbi.nlm.nih.gov/geo) with GEO number GSE41284.

SUPPLEMENTAL INFORMATION

Supplemental Information includes Extended Experimental Procedures, seven figures, and seven tables and can be found with this article online at http://dx.doi.org/10.1016/j.cell.2012.10.053.

ACKNOWLEDGMENTS

We thank H. Begthel, J. Korving, L. van Gurp, C. Kroon-Veenboer, and B. El Haddouti for technical assistance and T. Mahmoudi and J.D. Mul for their helpful discussions. This work was supported by Stichting Diabetes Onderzoek Nederland and the Diabetes Fonds. S.F.B. is supported by EMBO long-term fellowship (ALT-835-2007) and by EU/232814-stemcellmark; J.H.E. is supported by EU/232814-stemcellmark; V.S.W.L. is supported by KWF/PF HUBR 2007-3956; P.H. was supported by CGCII; A.H. was supported by KWF/PF HUBR 2007-3956; M.H. is supported by long-term Marie Curie fellowship and EU/236954-ICSC LGR5; M.B. is supported by Ti Pharm/T3-106; and A.J. and C.F. are supported by BIO2011-30299-C02-02 from MINECO and IIS10/00014 from Instituto de Salud Carlos III.

Received: September 1, 2011
Revised: September 11, 2012
Accepted: October 29, 2012
Published: December 20, 2012

REFERENCES

Apte, U., Zeng, G., Thompson, M.D., Muller, P., Micsenyi, A., Cieply, B., Kaestner, K.H., and Monga, S.P. (2007). beta-Catenin is critical for early postnatal liver growth. Am. J. Physiol. Gastrointest. Liver Physiol. *292*, G1578–G1585.

Benhamouche, S., Decaens, T., Godard, C., Chambrey, R., Rickman, D.S., Moinard, C., Vasseur-Cognet, M., Kuo, C.J., Kahn, A., Perret, C., and Colnot, S. (2006). Apc tumor suppressor gene is the "zonation-keeper" of mouse liver. Dev. Cell *10*, 759–770.

Cauchi, S., El Achhab, Y., Choquet, H., Dina, C., Krempler, F., Weitgasser, R., Nejjari, C., Patsch, W., Chikri, M., Meyre, D., and Froguel, P. (2007). TCF7L2 is reproducibly associated with type 2 diabetes in various ethnic groups: a global meta-analysis. J. Mol. Med. *85*, 777–782.

Clevers, H., and Nusse, R. (2012). Wnt/β-catenin signaling and disease. Cell *149*, 1192–1205.

da Silva Xavier, G., Loder, M.K., McDonald, A., Tarasov, A.I., Carzaniga, R., Kronenberger, K., Barg, S., and Rutter, G.A. (2009). TCF7L2 regulates late events in insulin secretion from pancreatic islet beta-cells. Diabetes *58*, 894–905.

Dashti, N., and Ontko, J.A. (1979). Rate-limiting function of 3-hydroxy-3-methylglutaryl-coenzyme A synthase in ketogenesis. Biochem. Med. *22*, 365–374.

de La Coste, A., Romagnolo, B., Billuart, P., Renard, C.A., Buendia, M.A., Soubrane, O., Fabre, M., Chelly, J., Beldjord, C., Kahn, A., and Perret, C. (1998). Somatic mutations of the beta-catenin gene are frequent in mouse and human hepatocellular carcinomas. Proc. Natl. Acad. Sci. USA *95*, 8847–8851.

Dor, Y., Brown, J., Martinez, O.I., and Melton, D.A. (2004). Adult pancreatic beta-cells are formed by self-duplication rather than stem-cell differentiation. Nature *429*, 41–46.

Eden, E., Navon, R., Steinfeld, I., Lipson, D., and Yakhini, Z. (2009). GOrilla: a tool for discovery and visualization of enriched GO terms in ranked gene lists. BMC Bioinformatics *10*, 48.

Elbein, S.C., Chu, W.S., Das, S.K., Yao-Borengasser, A., Hasstedt, S.J., Wang, H., Rasouli, N., and Kern, P.A. (2007). Transcription factor 7-like 2 polymorphisms and type 2 diabetes, glucose homeostasis traits and gene expression in US participants of European and African descent. Diabetologia *50*, 1621–1630.

Fechner, H., Haack, A., Wang, H., Wang, X., Eizema, K., Pauschinger, M., Schoemaker, R., Veghel, R., Houtsmuller, A., Schultheiss, H.P., et al. (1999). Expression of coxsackie adenovirus receptor and alphav-integrin does not correlate with adenovector targeting in vivo indicating anatomical vector barriers. Gene Ther. *6*, 1520–1535.

Ferré, P., Decaux, J.F., Issad, T., and Girard, J. (1986). Changes in energy metabolism during the suckling and weaning period in the newborn. Reprod. Nutr. Dev. *26*(2B), 619–631.

Ferrer, J.C., Favre, C., Gomis, R.R., Fernández-Novell, J.M., García-Rocha, M., de la Iglesia, N., Cid, E., and Guinovart, J.J. (2003). Control of glycogen deposition. FEBS Lett. *546*, 127–132.

Florez, J.C., Jablonski, K.A., Bayley, N., Pollin, T.I., de Bakker, P.I., Shuldiner, A.R., Knowler, W.C., Nathan, D.M., and Altshuler, D.; Diabetes Prevention Program Research Group. (2006). TCF7L2 polymorphisms and progression to diabetes in the Diabetes Prevention Program. N. Engl. J. Med. *355*, 241–250.

Grant, S.F., Thorleifsson, G., Reynisdottir, I., Benediktsson, R., Manolescu, A., Sainz, J., Helgason, A., Stefansson, H., Emilsson, V., Helgadottir, A., et al. (2006). Variant of transcription factor 7-like 2 (TCF7L2) gene confers risk of type 2 diabetes. Nat. Genet. *38*, 320–323.

Gregorieff, A., Grosschedl, R., and Clevers, H. (2004). Hindgut defects and transformation of the gastro-intestinal tract in Tcf4(-/-)/Tcf1(-/-) embryos. EMBO J. *23*, 1825–1833.

Gustafsson, J. (2009). Neonatal energy substrate production. Indian J. Med. Res. *130*, 618–623.

Hatzis, P., van der Flier, L.G., van Driel, M.A., Guryev, V., Nielsen, F., Denissov, S., Nijman, I.J., Koster, J., Santo, E.E., Welboren, W., et al. (2008).

Genome-wide pattern of TCF7L2/TCF4 chromatin occupancy in colorectal cancer cells. Mol. Cell. Biol. *28*, 2732–2744.

Huch, M., Gros, A., José, A., González, J.R., Alemany, R., and Fillat, C. (2009). Urokinase-type plasminogen activator receptor transcriptionally controlled adenoviruses eradicate pancreatic tumors and liver metastasis in mouse models. Neoplasia *11*, 518–528.

Korinek, V., Barker, N., Morin, P.J., van Wichen, D., de Weger, R., Kinzler, K.W., Vogelstein, B., and Clevers, H. (1997). Constitutive transcriptional activation by a beta-catenin-Tcf complex in APC-/- colon carcinoma. Science *275*, 1784–1787.

Korinek, V., Barker, N., Moerer, P., van Donselaar, E., Huls, G., Peters, P.J., and Clevers, H. (1998). Depletion of epithelial stem-cell compartments in the small intestine of mice lacking Tcf-4. Nat. Genet. *19*, 379–383.

Lieber, C.S. (1997). Cytochrome P-4502E1: its physiological and pathological role. Physiol. Rev. *77*, 517–544.

Lustig, B., Jerchow, B., Sachs, M., Weiler, S., Pietsch, T., Karsten, U., van de Wetering, M., Clevers, H., Schlag, P.M., Birchmeier, W., and Behrens, J. (2002). Negative feedback loop of Wnt signaling through upregulation of conductin/axin2 in colorectal and liver tumors. Mol. Cell. Biol. *22*, 1184–1193.

Lyssenko, V., Lupi, R., Marchetti, P., Del Guerra, S., Orho-Melander, M., Almgren, P., Sjögren, M., Ling, C., Eriksson, K.F., Lethagen, A.L., et al. (2007). Mechanisms by which common variants in the TCF7L2 gene increase risk of type 2 diabetes. J. Clin. Invest. *117*, 2155–2163.

Mokry, M., Hatzis, P., de Bruijn, E., Koster, J., Versteeg, R., Schuijers, J., van de Wetering, M., Guryev, V., Clevers, H., and Cuppen, E. (2010). Efficient double fragmentation ChIP-seq provides nucleotide resolution protein-DNA binding profiles. PLoS ONE *5*, e15092.

Párrizas, M., Maestro, M.A., Boj, S.F., Paniagua, A., Casamitjana, R., Gomis, R., Rivera, F., and Ferrer, J. (2001). Hepatic nuclear factor 1-alpha directs nucleosomal hyperacetylation to its tissue-specific transcriptional targets. Mol. Cell. Biol. *21*, 3234–3243.

Pilgaard, K., Jensen, C.B., Schou, J.H., Lyssenko, V., Wegner, L., Brøns, C., Vilsbøll, T., Hansen, T., Madsbad, S., Holst, J.J., et al. (2009). The T allele of rs7903146 TCF7L2 is associated with impaired insulinotropic action of incretin hormones, reduced 24 h profiles of plasma insulin and glucagon, and increased hepatic glucose production in young healthy men. Diabetologia *52*, 1298–1307.

Pilkis, S.J., and Granner, D.K. (1992). Molecular physiology of the regulation of hepatic gluconeogenesis and glycolysis. Annu. Rev. Physiol. *54*, 885–909.

Rojek, A.M., Skowronski, M.T., Füchtbauer, E.M., Füchtbauer, A.C., Fenton, R.A., Agre, P., Frøkiaer, J., and Nielsen, S. (2007). Defective glycerol metabolism in aquaporin 9 (AQP9) knockout mice. Proc. Natl. Acad. Sci. USA *104*, 3609–3614.

Sanderson, L.M., Degenhardt, T., Koppen, A., Kalkhoven, E., Desvergne, B., Müller, M., and Kersten, S. (2009). Peroxisome proliferator-activated receptor beta/delta (PPARbeta/delta) but not PPARalpha serves as a plasma free fatty acid sensor in liver. Mol. Cell. Biol. *29*, 6257–6267.

Savic, D., Ye, H., Aneas, I., Park, S.Y., Bell, G.I., and Nobrega, M.A. (2011). Alterations in TCF7L2 expression define its role as a key regulator of glucose metabolism. Genome Res. *21*, 1417–1425.

Saxena, R., Gianniny, L., Burtt, N.P., Lyssenko, V., Giuducci, C., Sjögren, M., Florez, J.C., Almgren, P., Isomaa, B., Orho-Melander, M., et al. (2006). Common single nucleotide polymorphisms in TCF7L2 are reproducibly associated with type 2 diabetes and reduce the insulin response to glucose in nondiabetic individuals. Diabetes *55*, 2890–2895.

Schuler, M., Dierich, A., Chambon, P., and Metzger, D. (2004). Efficient temporally controlled targeted somatic mutagenesis in hepatocytes of the mouse. Genesis *39*, 167–172.

Shu, L., Sauter, N.S., Schulthess, F.T., Matveyenko, A.V., Oberholzer, J., and Maedler, K. (2008). Transcription factor 7-like 2 regulates beta-cell survival and function in human pancreatic islets. Diabetes *57*, 645–653.

Shu, L., Matveyenko, A.V., Kerr-Conte, J., Cho, J.H., McIntosh, C.H., and Maedler, K. (2009). Decreased TCF7L2 protein levels in type 2 diabetes mellitus correlate with downregulation of GIP- and GLP-1 receptors and impaired beta-cell function. Hum. Mol. Genet. *18*, 2388–2399.

Spear, B.T., Jin, L., Ramasamy, S., and Dobierzewska, A. (2006). Transcriptional control in the mammalian liver: liver development, perinatal repression, and zonal gene regulation. Cell. Mol. Life Sci. *63*, 2922–2938.

van de Wetering, M., Cavallo, R., Dooijes, D., van Beest, M., van Es, J., Loureiro, J., Ypma, A., Hursh, D., Jones, T., Bejsovec, A., et al. (1997). Armadillo coactivates transcription driven by the product of the Drosophila segment polarity gene dTCF. Cell *88*, 789–799.

van de Wetering, M., Sancho, E., Verweij, C., de Lau, W., Oving, I., Hurlstone, A., van der Horn, K., Batlle, E., Coudreuse, D., Haramis, A.P., et al. (2002). The beta-catenin/TCF-4 complex imposes a crypt progenitor phenotype on colorectal cancer cells. Cell *111*, 241–250.

van Es, J.H., Haegebarth, A., Kujala, P., Itzkovitz, S., Koo, B.K., Boj, S.F., Korving, J., van den Born, M., van Oudenaarden, A., Robine, S., and Clevers, H. (2012). A critical role for the Wnt effector Tcf4 in adult intestinal homeostatic self-renewal. Mol. Cell. Biol. *32*, 1918–1927.

Weidinger, G., Thorpe, C.J., Wuennenberg-Stapleton, K., Ngai, J., and Moon, R.T. (2005). The Sp1-related transcription factors sp5 and sp5-like act downstream of Wnt/beta-catenin signaling in mesoderm and neuroectoderm patterning. Curr. Biol. *15*, 489–500.